Journal of
PERIODONTAL RESEARCH

J Periodont Res 2010; 45: 31–37

JOURNAL OF PERIODONTAL RESEARCH
doi:10.1111/j.1600-0765.2008.01199.x

Oral malodorous compound triggers mitochondrial-dependent apoptosis and causes genomic DNA damage in human gingival epithelial cells

B. Calenic, K. Yaegaki, T. Murata, T. Imai, I. Aoyama, T. Sato, H. Ii
Department of Oral Health, Nippon Dental University, Tokyo, Japan

Calenic B, Yaegaki K, Murata T, Imai T, Aoyama I, Sato T, Ii H. Oral malodorous compound triggers mitochondrial-dependent apoptosis and causes genomic DNA damage in human gingival epithelial cells. J Periodont Res 2010; 45: 31–37.

Background and Objective: Volatile sulfur compounds are the main compounds causing halitosis. One of these compounds, hydrogen sulfide (H_2S), which is responsible for physiological halitosis, is reported also to have periodontal pathogenic activities. Hydrogen sulfide has been shown to activate the apoptotic process in different tissues. Apoptosis plays an important role in the development of periodontitis. The aim of this study was to determine whether H_2S causes apoptosis in human gingival epithelial cells and to examine the cellular signaling pathway initiating the process.

Material and Methods: Human gingival epithelial cells were incubated with 50 ng/mL H_2S in air contining 5% CO_2 for 24, 48 or 72 h. To detect apoptosis, the cells were stained with annexin V and 7-amino actinomycin D, and analyzed using flow cytometry. Reactive oxygen species, mitochondrial membrane depolarization and release of cytochrome C into the cytosol were assessed using flow cytometry and enzyme-linked immunosorbent assay. Activity levels for the key apoptotic enzymes caspase-9, -8 and -3 were also determined. Genomic DNA damage was detected using single-cell gel electrophoresis.

Results: Apoptosis was significantly increased to 24.5 ± 5.7 at 24 h and 41.5 ± 8.9% at 48 h ($p < 0.01$). Reactive oxygen species were enhanced and mitochondrial membrane depolarization was collapsed. Cytochrome C release was dramatically increased (0.12 ± 0.02 vs. 0.02 ± 0.01 at 24 h and 0.21 ± 0.02 vs. 0.02 ± 0.01 ng/mL at 48 h; $p < 0.05$). Caspase-9 and -3 were strongly activated, while caspase-8 activity remained low. The percentage of DNA strand breaks increased, especially at 48 h.

Conclusion: Hydrogen sulfide induces apoptosis in human gingival epithelial cells by activating the mitochondrial pathway.

Ken Yaegaki, DDS, PhD, Department of Oral Health, Nippon Dental University, 1-9-20 Fujimi, Chiyoda-ku, Tokyo, 102-8159 Japan
Tel: +81 03 3261 8791
Fax: +81 03 3261 8796
e-mail: yaegaki-k@tky.ndu.ac.jp

Key words: hydrogen sulphide; periodontitis; apoptosis; halitosis

Accepted for publication December 5, 2008

'Oral malodor', the term used to describe offensive odors of the breath originating mostly from the oral cavity, is an increasing problem in today's society. Many compounds can be found in human breath air, but volatile sulfur compounds (VSCs) are the substances primarily responsible for oral malodor (1). The VSCs in the oral cavity are mainly hydrogen sulfide (H_2S) and methyl mercaptan (CH_3SH). Of the two, H_2S plays a distinct role in physiological halitosis (2).

Our previous research focused not only on the esthetic problems of VSCs but also on their toxicities. Studies have shown that increased levels of H_2S in the oral environment have a highly toxic effect on oral tissues and play a role in the etiology and development of periodontitis (3,4). The VSCs have been shown to alter the permeability of gingival tissues, thus facilitating the penetration of lipopolysaccharide into gingival epithelium and inducing inflammatory responses. Moreover, VSCs can increase the production of collagenase and prostaglandin E_2, both of which are key mediators in the processes of tissue destruction and inflammation. In studies focused on their effects on gingival connective tissue, we stress that VSCs inhibit collagen synthesis (5) and decrease total protein production by human gingival fibroblasts (6). In addition, VSCs interfere in the wound-healing process by inhibiting the proliferation of epithelial cells (7) and the synthesis of basal membranes (8). Collectively, these findings suggest that VSCs are periodontally pathogenic.

A number of recent studies have demonstrated the involvement of H_2S in the apoptotic process. Under normal conditions, apoptosis is essential for regulating tissues during embryogenesis and for maintaining normal homeostasis (9). Hydrogen sulfide may play a bifunctional role in cell survival; that is, while H_2S inhibits apoptosis in human polymorphonuclear neutrophils (10), lymphocytes (11) and cardiac myocytes (12), it may also stimulate apoptosis in human aorta smooth muscles cells (13), human lung fibroblasts (14) and/or pancreatic acinar cells (15). In the oral environment, however, the apoptotic effect of H_2S on human gingival cells has not been elucidated.

Detection of apoptosis in human gingival tissues indicates that it may play an important role in the development and control of inflammation and cell destruction in periodontal disease (16–19). Thus, programmed cell death might be one of the mechanisms involved in the pathogenesis of periodontitis. In a previous study, we showed that H_2S, at concentrations lower than those found in pathological gingival crevicular fluid, causes genomic DNA damage and apoptosis in human gingival fibroblasts (20). In the present study, we focus on the interrelationship of H_2S, apoptosis and gingival epithelial cells, since the gingival epithelial cells serve as the first line of defense against periodontal pathogens. We also examine the cellular signaling pathways implicated in the apoptotic process.

Material and methods

Cell culture

Cells from a human gingival epithelial cell line, Ca9-22 (Health Science Research Resources Bank, Osaka, Japan), were cultured in Dulbecco's modified Eagle's medium (Invitrogen, Carlsbad, CA, USA) supplemented with 10% fetal bovine serum (Invitrogen) at 37°C in an atmosphere of air containing 5% carbon dioxide (CO_2). For each experiment, the cells were plated in 25 cm^2 flasks at 4×10^5 cells well density and allowed to attach overnight. Prior to incubation, the cells were washed twice in prewarmed phosphate-buffered saline (PBS) and then placed in fresh medium. The prepared samples were placed in an H_2S incubation system and incubated in air contining 5% CO_2 mixed with H_2S (50 ng/mL) for 24, 48 or 72 h for apoptosis detection and 24 and 48 h for apoptotic pathway analysis. However, as a result of diffusion, the amount of H_2S in the medium was found to be only 18 ng/mL (0.5 μmol/L), a much lower concentration than the one found in gingival crevicular fluids from periodontal gingival tissues, which is 1.9 mmol/L H_2S as reported by Persson (21).

Negative control samples were subjected to an identical procedure, except that they were incubated in air containing CO_2 without H_2S.

Hydrogen sulfide incubation system

The H_2S incubation system allows incubation in a 37°C incubator with a H_2S sealed chamber. The 25 cm^2 flasks containing the Ca9-22 cells were placed inside the sealed chamber. A standard H_2S permeator (PD-1B-2; Gastec, Kanagawa, Japan), and H_2S permeation tubes (Permeacal; Gastec) were used to supply 5% CO_2 in H_2S at 50 ng/mL concentration in the chamber with a constant air flow of more than 200 mL/min.

Detection of apoptosis

For the detection of apoptosis and for distinguishing non-apoptotic from apoptotic cells, a Guava Nexin PCA (Guava Technologies, Hayward, CA, USA) was used. The method is based on double staining with two fluorescent dyes, allowing direct detection via flow cytometry. This assay includes annexin V for the detection of early apoptosis and 7-amino actinomycin D (7-AAD) as an indicator of late apoptosis or necrosis. annexin V binds phosphatidylserine translocated to the external membrane surface in early apoptotic cells (22), and 7-AAD, a DNA intercalator, permeates late-stage apoptotic and necrotic cells. After treatment with H_2S for 24 or 48 h, the cells were washed with PBS, trypsinized, pelleted and resuspended in cold Guava Nexin buffer at a concentration of 1×10^6 cells mL. Subsequently, the cells were double stained with 2.5 μL of 7-AAD and 5 μL of Annexin V-PE and immediately placed in ice for 20 min. For each experiment, 2000 cells were analyzed using Guava EasyCyte flow cytometry. Data acquisition and analysis were performed using Guava CytoSoft™ software.

Reactive oxygen species (ROS)

Oxidative stress was assessed through measurement of levels of ROS in the mitochondria using a red mitochon-

drial superoxide indicator (MitoSOX, Invitrogen). After tryspinization, the cells were centrifuged for 5 min at 1500 *g*. The supernatant was discarded, and the cells were resuspended in Dulbecco's PBS (with Ca^{2+} and Mg^{2+}) to a final concentration of 10^6 cells/mL. A 100 μL aliquot sample was then added, along with 1 mM MitoSOX reagent stock solution and 900 μL Dulbecco's PBS (with Ca^{2+} and Mg^{2+}) in a 1.5 mL test tube. The samples were incubated for 10 min at 37°C and then analyzed by flow cytometry.

Detection of mitochondrial membrane potential

Changes in mitochondrial membrane potential in H_2S-exposed epithelial cells were detected by Guava EasyCyte MitoPotential. The depolarization of the membrane was evaluated through measurement of the uptake of a cationic dye, 5,5′,6,6′-tetrachloro-1,1′,3,3′-tetraethyl-benzamidazolocarbocyanin iodide, commonly known as JC-1, into mitochondria. Collapse of the membrane potential initiates the early stages of the mitochondrial pathway-dependent apoptosis. In this assay, JC-1 fluoresces either green or orange, depending on mitochondrial membrane potential. The dye 7-AAD was used for monitoring cell membrane permeability associated with late apoptosis or necrotic cell death. After incubation with H_2S, the cells were trypsinized, pelleted and resuspended in 200 μL Dulbecco's MEM together with 2 μL JC-1 and 2 μL 7-AAD. The cells were incubated for 30 min in a 37°C CO_2 incubator and then analyzed for fluorescence by a flow cytometer.

Detection of cytochrome C

For analysis of cytochrome C release into the cytosol, subcellular fractionation was performed to separate the mitochondria from the cytosol, and only the cytosolic fraction was used in the assay. The assay (Cytochrome C ELISA, Calbiochem, San Diego, CA, USA) employed a quantitative sandwich enzyme immunoassay technique. Controls, samples and manufacturer-provided standards were pipetted into wells precoated with a monoclonal antibody specific for cytochrome C. After the cells were washed with PBS, an enzyme-linked monoclonal antibody specific for cytochrome C was added to all wells. Following another washing step, a substrate solution was added to wells. The color developed in proportion to the amount of cytochrome C bound in the first step. When color development was stopped, the optical density was determined using a microplate reader (Bio-Rad Benchmark Plus, Bio-Rad Japan, Tokyo, Japan) set to 450 nm with a wavelength correction set to 540 nm.

Caspase-3 activity assay

Caspase-3 activity was determined using a Caspase-3 Detection Kit (Oncogene Research Products, San Diego, CA, USA). The assay uses fluorescein isothiocyanate (FITC) as a fluorescent marker, conjugated with Asp-Glu-Val-Asp-*O*-methyl-fluoromethylketone (also known as DEVD-FMK), a cell-permeable caspase peptide inhibitor. The FITC–DEVD-FMK binds irreversibly to activated caspase-3 in apoptotic cells, and its FITC label allows for direct detection by a flow cytometer. After trypsinization and centrifugation, the cells were resuspended in PBS at a final concentration of 1×10^5 cells mL. A quantity of 300 μL of each sample, and a control sample was combined with 1 μL FITC–DEVD-FMK in microfuge tubes and incubated for 1 h in a 37°C incubator with air containing 5% CO_2. Subsequently, the cells were centrifuged for 5 min at 2500 *g*, the supernatant was removed, the cells were resuspended in 500 μL of washing buffer (prepared immediately before use), and the cells were again centrifuged for 5 min at 2500 *g*. The cells were then resuspended in 300 μL of washing buffer and analyzed via a Guava EasyCyte flow cytometer using the FL-1 standard channel.

Caspase-9 activity assay

For the detection of caspase-9 levels, a Caspase-9 Detection Kit (Calbiochem, San Diego, CA) was used. The assay uses a caspase-9 inhibitor, Leu-Glu-His-Asp-methyl-fluoromethylketone (LEHD-FMK), which binds irreversibly to activated caspase-9, and the fluorescent marker FITC. After tryspinzation and centrifugation, the concentration of the cells was adjusted to 1×10^5 cells mL using the technique described for the caspase-3 activity assay. The cells were then resuspended in 300 μL of washing buffer and analyzed by the Guava EasyCyte flow cytometer using the FL-1 standard channel.

Caspase-8 activity assay

To evaluate caspase-8 activity, a Caspase-8 Detection Kit (Calbiochem) was used. A synthetic caspase-8 inhibitor, Ile-Glu-Thr-Asp-methyl-fluoromethylketone (IETD-FMK), and FITC were used for this assay, allowing direct detection with a flow cytometer. After tryspinzation and centrifugation, the concentration of cells was adjusted to 1×10^5 cells mL using the technique described for the caspase-3 activity assay. The cells were then resuspended in 300 μL of washing buffer and analyzed by the Guava EasyCyte flow cytometer using the FL-1 standard channel.

Single-cell gel electrophoresis assay

Genomic DNA damage was detected using single-cell gel electrophoresis (Comet Assay; Trevigen, Gaithersburg, MD, USA), based on the principle that DNA has a highly organized structure which, in damaged DNA, is disrupted. When placed in an electric field, undamaged DNA strands migrate very slowly and remain confined within the nucleoid, compared with the small fragments of damaged DNA, which move much faster. When viewed under the microscope, the cell is shaped like a comet, its head corresponding to the nuclear region and its tail the damaged DNA fragments. The cells were suspended in PBS at a concentration of 1×10^5 cells/mL. Further, the cells were incorporated in agarose gel (LMAgarose; Trevigen). They were lysed using a lysis solution

and then placed in an electrophoretic field at a constant voltage of 1 V/cm for 10 min. The slides holding the samples (CometSlide; Trevigen) were placed in 70% ethanol for 5 min. After drying, the cells were stained using SYBR Green 1 (Trevigen). This was followed by image analysis using a fluorescence microscope. The images were obtained with a digital camera and processed using imaging software (TriTek CometScore, Sumerduck, VA, USA). For assessing the amount of DNA damage induced by H_2S, the following parameters were analyzed: tail length, which indicates the distance of damaged DNA migration from the nucleoid; percentage of DNA in the tail, which expresses the proportion of total DNA present in the tail; and tail moment, which represents the product of two values, namely the percentage of DNA in the comet tail and the tail length.

Statistical analysis

Results from five independent experiments are presented as the means ± SD. Statistical analysis was performed using one-way analysis of variance (ANOVA). Statistical significance was accepted at $p < 0.05$.

Results

Hydrogen sulfide-induced apoptosis

The percentage of apoptotic cells increased in a time-dependent manner. A significant difference in early apoptotic levels was found between test groups ($p < 0.01$, ANOVA). In addition, the number of early apoptotic cells was significantly increased after both 24 and 48 h compared with their control groups (24.5 ± 5.7 vs. 5.5 ± 2.3% after 24 h and 41.5 ± 8.9 vs. 4.1 ± 0.8% at 48 h of incubation; $p < 0.01$, ANOVA; Fig. 1A). After 24 and 48 h, late apoptotic and necrotic events were found to be < 5%. The data support the observation that the cells were in different stages of early apoptosis after 2 days of incubation with H_2S, and very few cells were in a late apoptotic or a necrotic stage. After 72 h, the percentage of necrosis and late apoptosis was significantly increased (40.6 ± 8.4 vs. 3.5 ± 1.9%; $p < 0.01$, ANOVA), while early apoptosis decreased to 10% of the total cell number (Fig. 1B).

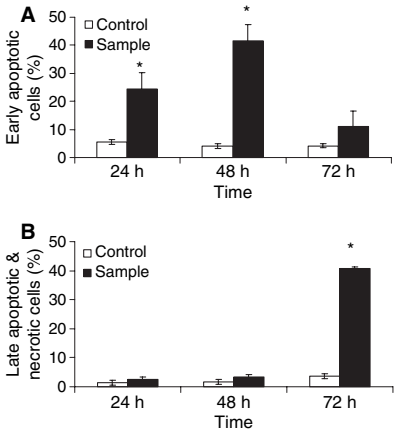

Fig. 1. Hydrogen sulfide triggers apoptosis in epithelial cells derived from human gingiva. Apoptosis levels were detected by flow cytometry after staining with Annexin V and 7-AAD. (A) Percentage of early apoptotic cells. After both 24 and 48 h, a significant difference was found between samples and their corresponding controls. After 72 h, early apoptosis was decreased. The data show that after 48 h of incubation, the main biological event was early apoptosis, with very few late apoptotic and necrotic cells. (B) Late apoptotic and necrotic cells. After 24 and 48 h, the presence of these cells was < 5% at each time point, while after 72 h the levels of necrosis and late apoptosis were greatly increased. Each bar represents the mean ± SD of 5 independent experiments (*$p < 0.05$ vs. control).

Mitochondrial changes

The mitochondrial apoptotic pathway is marked by profound changes in mitochondria. The presence of ROS in the mitochondria was detected according to the number of MitoSOX-positive cells in five independent experiments. A significant difference was observed after both 24 and 48 h between H_2S-incubated samples and their respective control groups (42.9 ± 9.5 vs. 7.6 ± 3.6% at 24 h and 56.6 ± 4.1 vs. 9.1 ± 3.7% at 48 h; $p < 0.01$, ANOVA; Fig. 2A). Another line of assessment relied on JC-1, a fluorescent dye that can monitor mitochondrial membrane depolarization. The percentage of membrane-depolarized cells was significantly increased at each time point compared with control groups (45.8 ± 11 vs. 14.5 ± 5% at 24 h and 38.1 ± 10.5 vs. 19.6 ± 5.5% at 48 h; $p < 0.01$, ANOVA; Fig. 2B). A key event in the intrinsic apoptotic pathway is the release of cytochrome C from the mitochondria. A significant increment of cytochrome C levels into cytosol was observed after both 24 and 48 h (0.12 ± 0.02 vs. 0.02 ± 0.01 ng/mL at 24 h and 0.21 ± 0.02 vs. 0.02 ± 0.01 ng/mL at 48 h; $p < 0.05$, ANOVA; Fig. 2C).

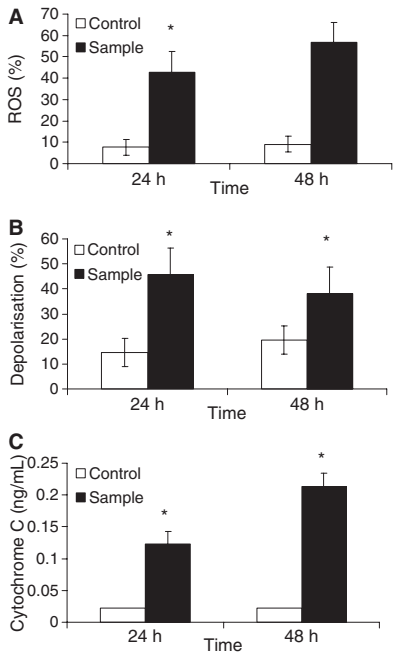

Fig. 2. Mitochondrial changes. (A) Reactive oxygen species, a marker of cellular stress, were significantly increased compared with control groups at each point of analysis. (B) Mitochondrial membrane electrical gradient was disrupted after both 24 and 48 h of H_2S incubation. (C) Release of cytochrome C from mitochondria into cytosol is a key event in the activation of the intrinsic apoptotic pathway. After both 24 and 48 h, release of cytochrome C into the cytosol was significantly increased compared with the corresponding control groups. Each bar represents the mean ± SD of 5 independent experiments (*$p < 0.05$ vs. control).

Caspase activities

Following H_2S incubation, caspase-9, an upstream regulator of the apoptotic process, was significantly activated compared with control groups (18.7 ± 3.8 vs. 5.3 ± 2.5% at 24 h and 51.1 ± 2.8 vs. 4.6 ± 1.1% at 48 h; $p < 0.01$, ANOVA; Fig. 3A). Significant differences were also found between caspase-3 activity levels in test groups compared with their control groups (25.6 ± 8.4 vs. 3.3 ± 1.1% at 24 h and 46.1 ± 8 vs. 3.0 ± 1.2% at 48 h; $p < 0.05$, ANOVA; Fig. 3B). At the same time, caspase-8 levels remained very low and were comparable to control groups, suggesting that the apoptotic process initiated by H_2S is independent of the extrinsic pathway (5.5 ± 2.1 vs. 4.5 ± 2.3% at 24 h and 7.0 ± 1.5 vs. 2.8 ± 2.1% at 48 h; Fig. 3C).

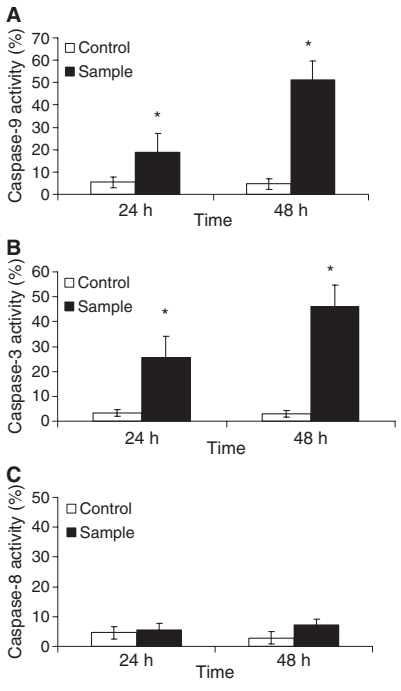

Fig. 3. Caspase activities. For caspase activity detection, FITC, a fluorescent marker allowing direct detection by a flow cytometer, was conjugated with caspase peptide inhibitors for caspase-9, -3 or -8. (A,B) Caspase-9 and -3 levels, respectively, were significantly increased compared with their control groups, suggesting that H_2S-induced apoptosis is activated via an intrinsic apoptotic pathway. (C) Caspase-8 activity remained low, comparable to the control group, proving the inactivity of the death-receptor apoptotic pathway. Each bar represents mean ± SD of 5 independent experiments (*$p < 0.05$ vs. control).

Genomic DNA damage

Using single-cell gel electrophoresis, we also observed the genotoxicity of H_2S by evaluating the DNA 'comet' tail shape. Tail length, percentage of DNA in tail, and their product, tail moment, are parameters correlated with the number of DNA strand breaks. All parameters were increased, suggesting significantly more DNA strand breaks in test groups than in the corresponding control groups: for tail length, 7.82 ± 2.94 vs. 1.97 ± 0.06 at 24 h and 16.71 ± 6.86 vs. 0.97 ± 0.06 at 48 h ($p < 0.05$, ANOVA; Fig. 4A); for DNA in tail, 12.92 ± 4.12 vs. 2.26 ± 0.08% at 24 h and 16.52 ± 4.14 vs. 2.73 ± 0.57% at 48 h ($p < 0.05$; Fig. 4B); and for tail moment, 1.51 ± 0.51 vs. 0.09 ± 0.05% at 24 h and 3.95 ± 0.72 vs. 0.11 ± 0.07% at 48 h ($p < 0.05$, ANOVA; Fig. 4C).

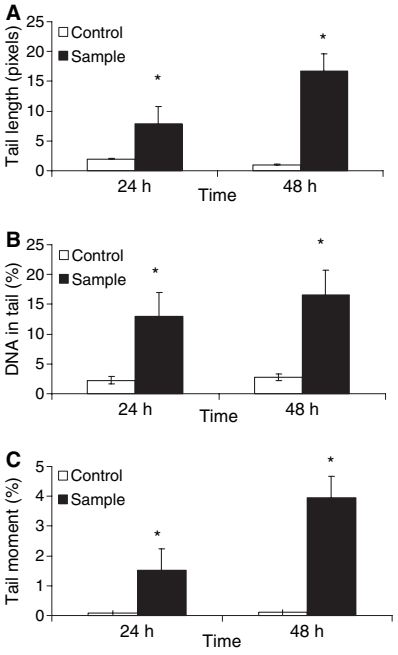

Fig. 4. Genomic DNA damage following hydrogen sulfide incubation. Genomic DNA damage was detected using single-cell gel electrophoresis and quantified using three different parameters. (A) Tail length, expressing distance of damaged DNA migration from the nucleoid, was significantly increased after 24 and 48 h compared with control cells. (B) Percentage of DNA in tail, showing the proportion of total DNA in tail, was increased after both 24 and 48 h. (C) Tail moment, representing the product of the first two parameters, was significantly increased at each time point compared with control groups. Each bar represents mean ± SD of 5 independent experiments; 75 nuclei analyzed per experiment (*$p < 0.05$ vs. control).

Discussion

Apoptosis, or programmed cell death, is a normal process in the development of multicellular organisms. Cells initiate the apoptotic process in response to a wide variety of stimuli; cell death is thus regulated and homeostasis maintained. Dysfunctions during the apoptotic process may lead to either prolonged cell survival or premature cell death. Therefore, excessive or insufficient apoptosis contributes to a wide range of human diseases, such as cancer, viral infections and degenerative disorders (23,24).

Studies of the relationship between apoptosis and the development of periodontal disease have shown that apoptosis plays a critical role in host immune response and inflammation, both of which are involved in periodontitis. Previous studies have reported apoptosis of polymorphonuclear leukocytes in gingival tissues with periodontitis (25,26). Periodontal disease leads to progressive degradation of connective tissue. Apoptosis among periodontal ligament fibroblasts increased in the early stages of periodontitis (27). Human gingival fibroblasts infected with *Porphyromonas gingivalis* for 24–36 h showed activation of the mitochondrial pathway and nuclear DNA degradation (28), while apoptotic inducers, such as butyric acid, caused apoptosis in gingival fibroblasts isolated from inflamed periodontal lesions (29). Gingival tissues in chronic periodontitis have increased apoptotic activity (16,28,30), while severe periodontitis is marked by a rise in the number of pro-apoptotic genes (31). Thus, apoptosis is actively involved in periodontal pathogenesis.

In healthy gingiva, oral epithelium plays a key role as a barrier against

pathogens or toxic compounds. The maintenance of this epithelial barrier is therefore extremely important for the preservation of normal gingival structure and function. However, during the progression of periodontal disease, this barrier can be affected. Several studies have focused on the relationship between oral malodorous compounds and this epithelial barrier. A study conducted by Tonzetich & Ng used a porcine model for gingival crevicular epithelia to show that exposure to concentrations of VSCs much lower than those found in periodontal pockets caused increased permeability of sublingual nonkeratinized mucosa (32). Another study, also conducted by Tonzetich and others, shows that VSCs can cause total disruption of the basement membrane (33). Furthermore, VSCs induced an important decrease in the collagen content of the VSC-exposed cell cultures (5,6). Other studies showed that increased concentrations of CH_3SH have an inhibitory effect on both cell growth and proliferation in human oral epithelial cell lines (34). Hydrogen sulfide was also shown to induce cell cycle arrest in oral epithelial cells, which may contribute to delayed epithelial repair (35). However, the apoptotic effect of H_2S on oral epithelial cells and the molecular mechanisms of this process remain unexplained. In the healthy epithelium, apoptosis occurs after basal keratinocytes mature and then differentiate. In the oral cavity, an enhanced apoptotic process may attenuate the barrier functions of epithelium against periodontally pathogenic strains of microorganisms or their products.

In the present study, we demonstrated that H_2S induces apoptosis in epithelial cells derived from human gingiva, and we identified the mechanisms underlying activation of the apoptotic signaling pathway. After 24 and 48 h incubation in a physiological concentration of H_2S, more than one-third of the cells were found to be in different stages of early apoptosis (20), whereas late apoptotic and necrotic levels were lower than 5%. Our data show that after 2 days of incubation, the main events caused by H_2S are features of early apoptosis. Apoptotic levels were also detected after 72 h. Necrosis and late apoptosis was dramatically increased at 72 h, while early apoptotic levels decreased to one-quarter of the 48 h incubation levels. Therefore, to analyze the apoptotic pathway we employed 24 and 48 h incubation times, since at both these time points the main cell death event was early apoptosis.

The two main mechanisms in the apoptotic process involve activation of an intrinsic pathway, in which the mitochondrion plays a central role, and activation of an extrinsic pathway, involving a receptor–ligand-mediated mechanism (36). To distinguish between the two pathways, we analyzed mitochondrial changes. Increased production of ROS in mitochondria causes disruption of the electrochemical gradient across the inner mitochondrial membrane, which then activates the apoptotic process (37). We found that H_2S increased ROS and caused a significant loss of the mitochondrial inner transmembrane potential. Collapse of this potential is associated with early stages of apoptosis; moreover, it leads to a key event in the mitochondrial pathway of apoptosis, that is, the release of cytochrome C from the mitochondria intermembrane into cytosol. In response to H_2S, the release of cytochrome C was significantly increased, especially after 48 h of incubation. In turn, cytochrome C release initiates the apoptotic caspase cascade by activating caspase-9, an initiator caspase responsible for the upstream regulation of apoptosis (38,39). In this study, caspase-9 levels were markedly increased. Exposure to H_2S also increased the activity of caspase-3, an executioner caspase responsible for the downstream regulation of the apoptotic process (40). Meanwhile, caspase-8 levels remained low and were comparable to control levels. Caspase-8 is an initiator caspase activated in the receptor–ligand-mediated apoptosis (41), and its inactivity suggests that the extrinsic pathway is not involved in H_2S-induced apoptosis.

Taken together, these results suggest that H_2S induces apoptosis by activating the mitochondrial intrinsic pathway (Fig. 5). In a previous study, H_2S was shown to induce genomic DNA damage in human gingival fibroblasts (20). Using a single-cell gel electrophoresis, we also observed an increment in the number of DNA strand breaks at the genomic level, proving the genotoxic effect of H_2S. Genomic DNA damage suggests that other molecular pathways, such as the p53 pathway, might be involved in the apoptotic process and that H_2S may have pathological effects on human gingiva at the genomic level.

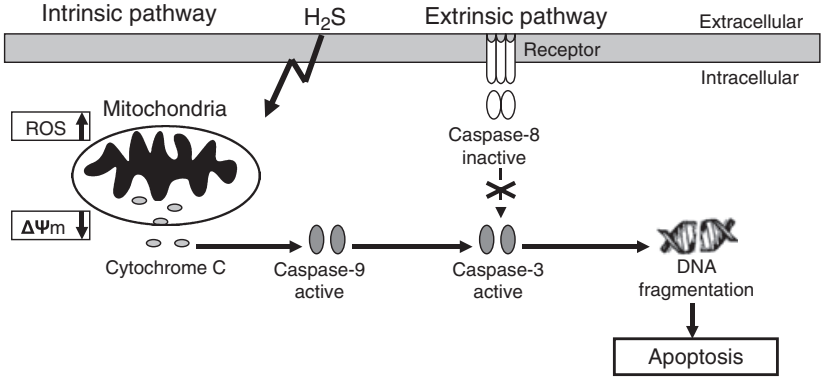

Fig. 5. Hydrogen sulfide triggers mitochondrion-dependent apoptosis via the intrinsic pathway. Hydrogen sulfide increases levels of ROS in the mitochondria and collapses the mitochondrial membrane potential ($\Delta\Psi_m$). These events are followed by release of cytochrome C from the mitochondria intermembrane into the cytosol. Cytochrome C activates caspase-9, an upstream caspase, which in turn activates caspase-3. Caspase-3 activation ultimately leads to DNA damage and apoptosis. Caspase-8 inactivity suggests that the extrinsic pathway is not involved in the process. For the techniques employed please refer to the 'Material and methods' section.

Acknowledgements

This research was supported by the grant-in-aid no. 203905380001 from the Japanese Ministry of Education, Culture, Sports, Science and Technology.

References

1. Oho T, Yoshida Y, Shimazaki Y *et al*. Characteristics of patients complaining of halitosis and the usefulness of gas chromatography for diagnosing halitosis. *Oral Surg Oral Med Oral Pathol Oral Radiol Endod* 2001;**91:**531–534.
2. Yaegaki K, Sanada K. Volatile sulfur compounds in mouth air from clinically healthy subjects and patients with periodontitis. *J Periodontal Res* 1992;**27:**233–238.
3. Rizzo A. Histologic and immunologic evaluation of antigen penetration into oral tissue after topical application. *J Periodontol* 1970;**41:**210–212.
4. Ratkay LG, Waterfield JD, Tonzetich J. Stimulation of enzyme and cytokine production by methyl mercaptan in human gingival fibroblast and monocytes cell cultures. *Arch Oral Biol* 1995;**40:**337–344.
5. Johnson P, Yaegaki K, Tonzetich J. Effect of methyl mercaptan on synthesis and degradation of collagen. *J Periodontal Res* 1996;**31:**323–329.
6. Johnson P, Yaegaki K, Tonzetich J. Effect of volatile thiol compounds on protein metabolism by human gingival fibroblasts. *J Periodontal Res* 1992;**27:**553–561.
7. Setoguchi T, Machigashira M, Yamamoto M *et al*. The effects of methyl mercaptan on epithelial cell growth and proliferation. *Int Dent J* 2002;**52:**241–246.
8. Yaegaki K. Oral malodor and periodontal disease. In: Rosenberg M, ed. *BAD BREATH: Research Perspectives*. Tel Aviv: Ramot Publishing-Tel Aviv University, 1995:87–108.
9. Raff M. Cell suicide for beginners. *Nature* 1998;**396:**119–122.
10. Mariggio MA, Minunno V, Riccardi S, Santacroce R, De Rinaldis P, Fumarulo R. Sulfide enhancement of PMN apoptosis. *Immunopharmacol Immunotoxicol* 1998;**20:**399–408.
11. Rinaldi L, Gobbi G, Pambianco M, Micheloni C, Mirandola P, Vitale M. H_2S prevents apoptosis of human PMN via inhibition of p38 and caspase 3. *Lab Invest* 2006;**86:**391–397.
12. Sivarajah A, Collino M, Yasin M *et al*. Anti-apoptotic and anti-inflammatory effects of hydrogen sulfide in a rat model of regional myocardial I/R. *Shock* 2008;[Epub ahead of print].
13. Yang G, Sun X, Wang R. H_2S induced-apoptosis of human aorta smooth muscle cells via activation of mitogen-activated protein kinases and caspase-3. *FASEB J* 2004;**18:**75–80.
14. Baskar R, Li L, Moore PK. H_2S induces DNA damage and changes in apoptotic gene expression in human lung fibroblast cells. *FASEB J* 2007;**21:**247–255.
15. Cao Y, Adhikari S, Ang AD, Moore PK, Bhatia M. Mechanism of induction of pancreatic acinar cell apoptosis by H_2S. *Am J Physiol Cell Physiol* 2006;**291:**C503–C510.
16. Leung WK, Wu Q, Hannam PM, McBride BC, Uitto V-J. *Treponema denticola* may stimulate both epithelial proliferation and apoptosis through MAP kinase signal pathways. *J Periodontal Res* 2002;**37:**445–455.
17. Jewett A, Hume WR, Le H *et al*. Induction of apoptotic cell death in peripheral blood mononuclear and polymorphonuclear cells by an oral bacterium, *Fusobacterium nucleatum*. *Infect Immun* 2000;**68:**1893–1898.
18. Gamonal J, Bascones A, Acevedo A, Blanco E, Silva A. Apoptosis in chronic adult periodontitis analyzed by in situ DNA breaks, electron microscopy, and immunochemistry. *J Periodontol* 2001;**72:**517–525.
19. Maurizio S, Cortellini D, Lang N. In situ detection of apoptosis at sites of chronic bacterially induced inflammation in human gingiva. *Infect Immun* 1998;**66:**5190–5195.
20. Yaegaki K, Qian W, Murata T *et al*. Oral malodorous compound causes apoptosis and genomic DNA damage in human gingival fibroblasts. *J Periodontal Res* 2008;**43:**391–9.
21. Persson S. H_2S and methyl mercaptan in periodontal pockets. *Oral Microbiol Immunol* 1992;**7:**378–379.
22. van England M, Nieland LJ, Ramaekers FC, Schutte B, Reutelingsperger CP. Annexin V-affinity assay: a review on an apoptosis detection system based on phosphatidylserine exposure. *Cytometry* 1998;**31:**1–9.
23. Debatin KM. Apoptosis pathways in cancer and cancer therapy. *Cancer Immunol Immunother* 2004;**53:**153–159.
24. Friedlander RM. Apoptosis and caspases in neurodegenerative diseases. *N Engl J Med* 2003;**348:**1365–1375.
25. Sawa T, Nishimura F, Ohyama H, Takahashi K, Takashiba S, Murayama Y. In vitro induction of activation-induced cell death in lymphocytes from chronic periodontal lesions by exogenous Fas ligand. *Infect Immun* 1999;**67:**1450–1454.
26. Koulouri O, Lappin DF, Radvar M, Kinane DF. Cell division, synthetic capacity and apoptosis in periodontal lesions analyzed by in situ hybridization and immunohistochemistry. *J Clin Periodontol* 1990;**26:**552–559.
27. Ekuni D, Tomofuji T, Yamanaka R, Tachibana K, Yamamoto T, Watanabe T. Initial apical migration of junctional epithelium in rats following application of lipopolysaccharide and proteases. *J Periodontol* 2005;**76:**43–48.
28. Urnowey S, Ansai T, Bitko V, Nakayama K, Takehara T, Barik S. Temporal activation of anti- and pro-apoptotic factors in human gingival fibroblasts infected with the periodontal pathogen, *Porphyromonas gingivalis*: potential role of bacterial proteases in host signaling. *BMC Microbiol* 2006;**8:**6.
29. Kurita-Ochiai T, Seta S, Suzuki N *et al*. Butyric acid induces apoptosis in inflamed fibroblasts. *J Dent Res* 2008;**87:**51–55.
30. Ekuni D, Tomofuji T, Yamanaka R, Tachibana K, Yamamoto T, Watanabe T. Caspase activation is involved in chronic periodontitis. *FEBS Lett* 2005;**579:**5559–5564.
31. Bulut S, Uslu H, Ozdemir BH, Bulut OE. Expression of caspase-3, p53, and Bcl-2 in generalized aggressive periodontitis. *Head Face Med* 2006;**2:**17.
32. Ng W, Tonzetich J. Effect of hydrogen sulfide and methyl mercaptan on the permeability of oral mucosa. *J Dent Res* 1984;**63:**994–997.
33. Johnson PW, Ng W, Tonzetich J. Modulation of human gingival fibroblast cell metabolism by methyl mercaptan. *J Periodontal Res* 1992;**27:**476–483.
34. Setoguchi T, Machigashira M, Yamamoto M *et al*. The effects of methyl mercaptan on epithelial cell growth and proliferation. *Int Dent J* 2002;**52**(Suppl 3)**:**241–246.
35. Takeuchi H, Setoguchi T, Machigashira M, Kanbara K, Izumi Y. Hydrogen sulfide inhibits cell proliferation and induces cell cycle arrest via an elevated p21 Cip1 level in Ca9-22 cells. *J Periodontal Res* 2008;**43:**90–95.
36. van Cruchten S, van den Broeck W. Morphological and biochemical aspects of apoptosis, oncosis and necrosis. *Anat Histol Embryol* 2002;**31:**214–223.
37. Green DR, Reed JC. Mitochondria and apoptosis. *Science* 1998;**281:**1309–1312.
38. Hill MM, Adrain C, Martin SJ. Portrait of a killer: The mitochondrial apoptosome emerges from the shadows. *Mol Interv* 2003;**3:**19–26.
39. Bossy-Wetzel E, Newmeyer DD, Green DR. Mitochondrial cytochrome-c release in apoptosis occurs upstream of DEVD-specific caspase activation and independently of mitochondrial transmembrane depolarization. *EMBO J* 1998;**17:**37–49.
40. Porter AG, Janicke RU. Emerging roles of caspase-3 in apoptosis. *Cell Death Differ* 1999;**6:**99–104.
41. Hengartner M. The biochemistry of apoptosis. *Nature* 2000;**407:**770–776.